Mon. Not. R. Astron. Soc. **000**, 1–?? (0000) Printed 30 July 2015 (MN LaTeX style file v2.2)

Constraining the formation of black-holes in short-period Black-Hole Low-Mass X-ray Binaries

Serena Repetto[1⋆], Gijs Nelemans[1,2]
[1]*Department of Astrophysics/IMAPP, Radboud University Nijmegen, P.O. Box 9010, 6500 GL Nijmegen, The Netherlands*
[2] *Institute for Astronomy, KU Leuven, Celestijnenlaan 200D, 3001 Leuven, Belgium*

30 July 2015

ABSTRACT
The formation of stellar mass black holes is still very uncertain. Two main uncertainties are the amount of mass ejected in the supernova event (if any) and the magnitude of the natal kick the black hole receives at birth (if any). Repetto et al. (2012), studying the position of Galactic X-ray binaries containing black holes, found evidence for black holes receiving high natal kicks at birth. In this Paper we extend that study, taking into account the previous binary evolution of the sources as well. The seven short-period black-hole X-ray binaries that we use, are compact binaries consisting of a low-mass star orbiting a black hole in a period less than 1 day. We trace their binary evolution backwards in time, from the current observed state of mass-transfer, to the moment the black hole was formed, and we add the extra information on the kinematics of the binaries. We find that several systems could be explained by no natal kick, just mass ejection, while for two systems (and possibly more) a high kick is required. So unless the latter have an alternative formation, such as within a globular cluster, we conclude that at least some black holes get high kicks. This challenges the standard picture that black hole kicks would be scaled down from neutron star kicks. Furthermore, we find that five systems could have formed with a non-zero natal kick but zero mass ejected (i.e. no supernova) at formation, as predicted by neutrino-driven natal kicks.

Key words: X-rays: binaries – supernovae: general – Galaxy: dynamics – binaries: general – black hole physics

1 Introduction

Since the discovery of the first stellar-mass black hole (BH) in the Galactic X-ray source Cygnus X-1 (Bowyer et al. 1965), other BHs have been found. Stellar-mass† BHs have a mass between ~ 5 and 30 times the mass of the Sun, while the peak of the Galactic distribution is centered at 8 $M_\odot$ (Özel et al. 2010). Their Galactic population currently amounts to 17 dynamically confirmed BHs (Casares & Jonker 2014), and 31 BH candidates (Tetarenko, B.E. et al. 2015, in prep).

So far, the best way to detect BHs is when they are actively accreting from a stellar companion, whose matter falls in the gravitational field of the BH while forming an accretion disc. We wish to mention the recent discovery of a BH with a Be-type star as companion (Casares et al. 2014). This system, in which the accretion flow onto the BH is radiatively inefficient, opens-up the possibility of a new detection-window for BHs. In black-hole low-mass X-ray binaries (BH-LMXBs), a BH accretes matter from a star similar in mass to our Sun. At some point in the evolution of the progenitor of a BH-LMXB, the companion overfills its Roche lobe, either because of its own nuclear expansion, or due to shrinking of the orbit caused by angular momentum losses. The material hence escapes the gravitational pull from the star and forms an accretion disc around the BH, which is detectable in the X-ray band (Shakura & Sunyaev 1973).

Despite the strong evidence for the existence of BHs, the way they actually form is still a matter of great debate. It is generally accepted that BHs are formed from the gravitational collapse of a massive star, a star with a mass on the main sequence (MS) greater than $20 - 25$ $M_\odot$, and/or a core mass greater than 8 $M_\odot$, e.g. Fryer (1999), MacFadyen et al. (2001), Tauris & van den Heuvel (2006). In one scenario, massive BHs are thought to form by direct collapse, whereas the lightest ones via fallback onto the nascent neutron star (NS). Two main uncertainties are the size of the velocity the BH receives at birth (*natal kick*, NK), if any, and the amount of mass ejected at the moment of BH formation, if any. These are the questions we address in this Paper.

Measuring BH natal kicks is of great importance for a number of reasons. First of all, the magnitude of the NK is dependent upon the physical mechanism driving the kick. For instance, if BHs were discovered to receive high kicks, this would have important implications for the supernova (SN) mechanism. Theoretical calculations by Janka (2013) show that the momentum of the BH can

⋆ E-mail: s.repetto@astro.ru.nl
† Throughout this Paper, we will refer to stellar-mass BHs simply as BHs.

grow with the fallback mass and lead to high kicks. Secondly, the velocity that BHs receive at birth affects the number of BHs which can be retained in a globular cluster (GC, Strader et al. 2012, Sippel & Hurley 2013, Morscher et al. 2015), as well as in a young stellar cluster (Goswami et al. 2014). Furthermore, the black hole NK distribution is an important ingredient in binary population synthesis (BPS) studies, for examples the ones which compute the gravitational wave (GW) merger rate of binaries harboring BHs (see for example Lipunov et al. 1997 and Dominik et al. 2015). Additionally, the likelihood of discovering isolated (and nearby) BHs accreting from the interstellar medium (ISM) through radio signatures detectable by future surveys, is a function of the BH velocity relative to the ISM, hence of the NK (Fender et al. 2013).

In our first study of BH natal kicks (Repetto et al. 2012), we found evidence for BHs receiving *high* kicks, where *high* stands for kicks similar to those received by NSs (that is, hundreds of km/s). In that study, high NKs were needed in order to match the current out-of-the-plane distribution of BH X-ray binaries.

As currently observed binary properties (e.g., orbital period, masses, and position in the Galactic potential) are determined by the conditions present at the moment of BH formation, and therefore significantly affected by the magnitude of both the ejected mass and NK imparted, BH-LMXB systems are the optimal tool for shedding light on BH formation mechanisms.

In this Paper, we focus on a subset of BH-LMXBs, those ones with a short orbital period (less than 1 day). In these systems the current mass transfer phase is driven by angular momentum loss in the form of magnetic braking (MB). This study is complementary to the study of Repetto et al. (2012) (Paper I hereafter). Contrary to Paper I, which used a BPS approach to study the NK magnitude required to explain the current out-of-plane distribution of Galactic BH-LMXBs, in this Paper we use a detailed binary evolution approach, allowing us to take into account the current orbital parameters of each system. We trace the binary evolution of the seven short-period BH-LMXBs backwards in time until the moment the BH was formed. This allows us to set constraints on the mass ejected and the NK in terms of lower limits.

Previous works on BH natal kicks combined the study of the binary evolution of the systems with the information on the space velocity. A small NK has been found for GRO J1655-40 (Willems et al. 2005) and for Cygnus X-1 (Wong et al. 2012), whereas evidence for a high NK was found for XTE J1118+480 (Fragos et al. 2009). Evidence for a BH formed in a SN explosion comes from the chemical enrichment in the spectra of the companion to the BH in XTE J1118+480 (González Hernández et al. 2006), in GRO J1655-40 (Israelian et al. 1999), in 1A 0620-00 (González Hernández et al. 2004), in V4641 Sgr (Orosz et al. 2001), and in V404 Cyg (González Hernández et al. 2011). Whereas Cygnus X-1 was claimed to have formed without a SN (Mirabel & Rodrigues 2003).

The Paper is structured as follows: in Section 2 we give a brief overview of the evolution of BH-LMXBs and of what we know about BH formation, in Section 3 we show the properties of the observed systems. In Section 4 we describe our method to calculate the NK and mass ejected for the seven binaries, and in Section 5 the results. We end with a discussion and conclusion of our findings.

2 A short overview of the evolution of BH-LMXBs

The standard formation scenario for a BH-LMXB is an extension of the formation scenario which explains low-mass X-ray binaries with a NS as accretor (van den Heuvel 1983). The primordial binary from which a neutron-star low-mass X-ray binary originates, is a binary with a very extreme mass ratio between the two components. In order to form a BH low-mass X-ray binary, one just needs to start with a more massive progenitor which will core-collapse into a BH, instead of a NS (Romani 1996, Portegies Zwart et al. 1997, Ergma & Fedorova 1998). The progenitor of a BH low-mass X-ray binary probably consists of a Sun-like star orbiting around a massive star (with a mass of $20 - 25\ M_{\odot}$). Typical orbital separations which allow a sun-like star to overfill its Roche lobe and transfer mass to a BH are of the order of $\sim 10\ R_{\odot}$. These separations are much smaller than the typical orbital separation that the progenitor of the BH-LMXB must have had in order to accommodate the progenitor of the BH during its nuclear expansion. Therefore, it is commonly accepted that the binary must have undergone a phase of common envelope (CE), which shrank the binary down by a factor of ~ 100 (Paczynski 1976). During the CE, the massive star is believed to lose its H-envelope; what is left, the Helium core, collapses into a BH. If the binary survives the event in which the BH forms, its further evolution can follow two alternative paths. The evolution can be driven by the nuclear evolution of the stellar component, and the binary will undergo mass transfer when the star is large enough for some of its material to fall in the gravitational potential of the BH. At the current state, the companion star is thus an evolved star off the MS. Alternatively, the evolution can be driven by angular momentum losses from the binary and the two components get closer and closer to each other thanks to the coupled effect of tides and magnetic braking, until mass transfer sets in. The latter ones are the binaries we focus on in this study, where the companion star is a MS-star. For previous studies of the evolution of BH-LMXBs see e.g. Ergma & Fedorova (1998), Kalogera (1999), Podsiadlowski et al. (2003), Yungelson et al. (2006).

2.1 Black hole formation and natal kicks at birth

In the most common scenario of BH formation, higher mass BHs are thought to form via direct collapse of the progenitor star, lighter mass BHs via fallback onto the proto-NS (Fryer & Kalogera 2001, MacFadyen et al. 2001, Heger et al. 2003, Zhang et al. 2008). BH formation via fallback occurs in a successful but weak explosion, where some fraction of the ejecta does not have enough kinetic energy to escape the potential well of the proto NS. However, we wish to highlight that the occurrence of fallback is not agreed upon by the entire SN community. Some studies showed that the fallback requires a fine-tuning between the explosion energy and the envelope binding energy (see for example Dessart et al. 2010). Normally, either the SN is successful and leads to the formation of a NS, or it is unsuccessful and all the material collapses into a BH. The BH mass would therefore be equal to the mass of the collapsing Helium core (see Kochanek 2015 and Clausen et al. 2015).

A further source of uncertainty is whether BHs receive NKs at birth or not, and what the size of the NK would be. There are two types of BH natal kicks, kicks (i) imparted intrinsically to the BH, and (ii) received as an effect of the NK imparted to the NS that forms a BH through fallback. The intrinsic kicks could be caused either by asymmetric gravitational wave emission during the core-collapse (Bonnell & Pringle 1995), or by asymmetric flux of those neutrinos which get to escape before all the collapsing material falls inside the event horizon (Gourgoulhon & Haensel 1993). In either cases, there is no need for mass-ejection at BH formation.

There are two main processes which are thought to cause NS natal kicks and are therefore relevant for BH formation via fallback:

either asymmetries in the SN ejecta (*ejecta-driven*, also called *hydrodynamical* NKs), or asymmetries in the neutrino flux (*neutrino-driven* NKs). Both of these two NK mechanisms have their own drawbacks (Fryer & Kusenko 2006). Only 1% of the collapse energy is in the ejecta, thus the hydrodynamics of the explosion has to develop a large degree of anisotropy to impart the NS a large NK. Instead, most of the energy and momentum liberated in the explosion are carried away by neutrino, hence only a small degree of asymmetry ($\sim$ 1%) in the neutrino flux is necessary to impart the NS a NK as high as hundreds km/s. However, this mechanism requires a strong magnetic field.

If the BH is formed via fallback onto the proto NS, the magnitude of the NK it receives depends on the competition between two timescales: the timescale for (some of) the material in the ejecta to fall back onto the nascent NS, $\tau_{\rm fb}$, and the timescale for the process which imparts the NS a NK, $\tau_{\rm NK}$. If $\tau_{\rm fb} > \tau_{\rm NK}$ we expect the BH to receive a reduced NK. If $\tau_{\rm fb} < \tau_{\rm NK}$, we expect the BH to receive a full NK. While hydrodynamic simulations by MacFadyen et al. (2001) show that fallback onto the NS happens within 100 s after core collapse, the timescale of NKs induced by neutrino emission and by hydrodynamics in the ejecta is estimated to be $\tau_{\rm NK} \sim 10$ s and $\tau_{\rm NK} \sim 0.1$ s respectively (Lai et al. 2001). This indicates that, in the fallback scenario, the BH would receive a reduced NK.

Just by conserving linear momentum, we expect reduced NKs to be of the order of $V_{\rm NK,BH} \sim (M_{\rm NS}/M_{\rm BH})\, V_{\rm NK,NS}$, leading the BH to receive a NK of the order of tens km/s. If this scenario is correct, we should find a correlation between the mass of the BH and the NK: the larger the BH mass, the larger the fallback mass, the lower the NK. We wish to highlight, however, that Janka (2013) suggests BHs could be accelerated to the same velocity as NSs, even in a fallback-scenario, due to the anisotropic gravitational pull from the asymmetrically expelled ejecta. Thus, in this scenario, BHs would receive high kicks even when $\tau_{\rm fb} > \tau_{\rm NK}$, and the momentum of the BH would grow with the fallback mass.

For NSs there is both evidence for high and low kicks. The proper motion of isolated pulsars implies transverse velocities up to 1000 km/s, with a mean birth speed for young pulsars of $\sim$ 400 km/s (Hobbs et al. 2005). On the other hand, few Galactic NS high-mass X-ray binaries seem to be more consistent with a low NK. These binaries have long periods and small eccentricities. Such a small eccentricity, being a prior of the eccentricity immediately after the SN explosion, requires a small NK, of the order of few tens km/s (Pfahl et al. 2002b). High NS natal kicks are thought to be produced in a standard core-collapse SN, whereas low NS natal kicks are thought to be produced in a less-energetic type of SN, an electron-capture SN from a low-mass star (Podsiadlowski et al. 2004). Such a low-mass star has little chance of forming a BH. When the collapsing core is low in mass, the explosion is thought to be so rapid that there is no time for large asymmetries to develop. Such a theoretical scenario is consistent with the results obtained tracing backwards the orbital properties of a few members of the Galactic population of double NS binaries (Wong et al. 2010). Few of them are consistent with a low-mass progenitor and a low NK at birth. The retention of NSs in GCs is another argument in favor of some NSs receiving low kicks (Pfahl et al. 2002a).

3 The Galactic population of short-period black-hole low-mass X-ray binaries

3.1 Orbital properties

In our Galaxy there are 13 BH-LMXBs with BH masses dynamically measured (Orosz et al. 2004, McClintock & Remillard 2006). Dynamical measurement of the BH mass is done tracing the Keplerian motion of the companion star. In this way, the BH mass can be determined once the orbital period, the radial velocity semi-amplitude of the companion star, the mass-ratio, and the inclination of the binary with respect to the line of sight, are known. The BH mass is a strong function of the inclination, hence it is the inclination the major contributor to any uncertainties in the BH mass. The inclination is typically determined fitting the ellipsoidal modulations in the optical light curve of the companion. The companion can be detected when the binary is in quiescence, i.e. when the accretion disc is under-luminous. Failure in accurately determining the contribution of the disc to the light curve, results in inaccurate BH mass determination. For an up-to-date overview of dynamical mass determinations in BHs, and the associated main sources of systematic errors, see Casares & Jonker (2014).

In Fig. 1 we show the orbital period $P_{\rm orb}$ of BH-LMXBs as a function of the mass of the companion $M_\star$. They fall in three categories: 10 short-period ($P_{\rm orb} \lesssim 1$ day) systems, of which 7 with $M_\star \lesssim 1.5\ M_\odot$, and 3 systems with longer periods. Out of this sample, we only consider the short-period binaries with low-mass companions. We don't consider the binary with 1.5 day period as a short-period binary, since it contains a giant as a companion (Orosz et al. 2011), so it is thought to evolve to longer periods.

The choice $P_{\rm orb} \lesssim 1$ day is motivated by the fact that binaries with longer periods are driven by the evolution of the donor, while only those with shorter periods are driven by magnetic braking and evolve towards smaller and smaller periods until the companion overfills its Roche lobe, while still being on the MS (see Yungelson et al. 2006). This defines a so-called bifurcation period $P_{\rm bif}$ (Tutukov et al. 1985, Pylyser & Savonije 1989), that is shown as the solid line in Fig. 1. We calculate $P_{\rm bif}$ as the the orbital period such that the magnetic braking time scale ($\tau_{\rm MB}$, calculated below in Section 4.2.1) is equal to the main-sequence life-time. The limit $M_\star \lesssim 1.5\ M_\odot$ is motivated by the fact that more massive donors are not thought to sustain a significant surface magnetic field, hence magnetic braking is not supposed to operate. We wish to mention that Justham et al. (2006) proposed that BH-LMXBs could descend from a population of intermediate-mass X-ray binaries with Ap/Bp-star companions. However, the spectral types predicted by the stellar evolutionary tracks are too hot for explaining the observed temperatures of companion stars in BH-LMXBs.

We indicate the dynamical properties of the seven short-period BH X-ray binaries in Table 1. We wish to note that GRS 1009-45 lacks strong constraints on the mass of the BH. This is due to the large uncertainty on the inclination of the system, and the BH-mass value given in Filippenko et al. (1999) is a lower-limit (see Casares & Jonker 2014). Another BH-LMXB whose observational properties are debated is GRO J0422+32. Reynolds et al. (2007) claimed that negligible contamination arising from the accretion disc was assumed in the estimate from Gelino & Harrison (2003). They estimate the contamination to the companion-star light curve due to the accretion disc, and they get a lower limit to the BH mass of $\sim 10.4\ M_\odot$. Although both the reported masses are probably biased, because of very large flickering amplitude in the light curves (Casares & Jonker 2014), we find the measurement by Gelino & Harrison (2003) as the most reliable one, because it is based on a

Table 1. Dynamical properties of short-period black-hole low-mass X-ray binaries.

Source	$P_{\rm orb}$ [day]	$M_\star$ $[M_\odot]$	$M_{\rm BH}$ $[M_\odot]$	Ref.
XTE J1118+480	0.17	0.15-0.29	8.16-8.58	[1]
GRO J0422+32	0.21	0.15-0.77	3.02-4.92	[2]
GRS 1009-45	0.28	0.61^a	4.4^a	[3]
1A 0620-00	0.32	0.39-0.41	6.44-6.84	[4]
GS 2000+251	0.34	0.16-0.47	5.5-8.8	[5]
Nova Mus 91	0.43	0.68-0.81	6.35-7.55	[6]
H 1705-250	0.52	0.3-0.6	6.4-6.9	[7]

(a) This system lacks strong constraints on the component masses (see Text).
References: [1] González Hernández et al. (2012), [2] Gelino & Harrison (2003), [3] Filippenko et al. (1999), [4] González Hernández et al. (2014), [5] Ioannou et al. (2004), [6] Gelino et al. (2001), [7] Filippenko et al. (1997).

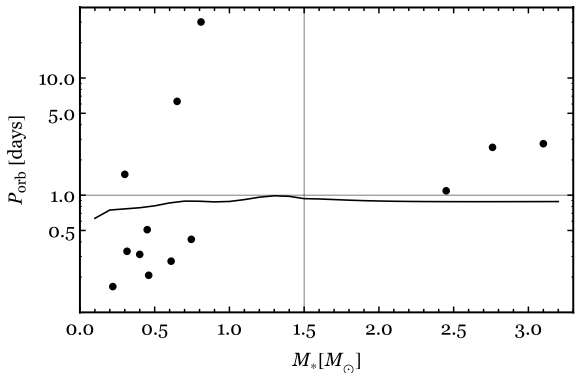

Figure 1. Black-hole low-mass X-ray binaries as a function of orbital period $P_{\rm orb}$ and companion mass $M_\star$. The solid line shows the bifurcation period. The sources in the bottom left of the plot are those we study in this work.

database where the ellipsoidal modulation is best detected. Neglecting the disc contribution to the light curve would, in any case, underestimate the inclination, and consequently overestimate the BH mass, in strong contrast with the results of Reynolds et al. (2007).

3.2 Mass-radius relation

For our sample, the companion star is currently overfilling its Roche lobe. From the observed binary properties and inferred masses we can hence calculate the radius of the companion assuming $R_\star = R_{\rm L}$, where $R_{\rm L}$ is the Roche lobe radius of the companion star (Eggleton 1983). The results are plotted in Fig. 2 and can be compared to the radii of single main sequence stars shown as the solid lines. We compute such radii for single stars, both at the beginning and at the end of the MS, with the SSE code by Hurley et al. (2000) embedded in the Astrophysics Multipurpose Software Environment AMUSE (Portegies Zwart et al. 2009).

As is well known, stars in interacting binaries are typically somewhat larger than single stars. This can be caused by the fact that the star does not have time to relax back to its thermal equilibrium (Knigge et al. 2011). In case one component is a NS or BH the effect of X-ray irradiation, which heats up (hence bloats) the star, can play a role (Podsiadlowski 1991, Harpaz & Rappaport 1991).

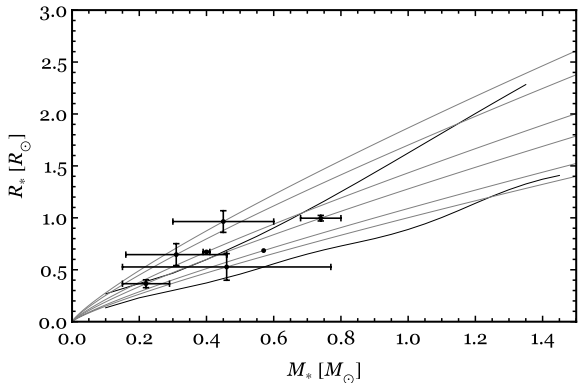

Figure 2. Radius and mass of the seven short-period black-hole low-mass X-ray binaries. The two black lines correspond to the radius of single stars at the beginning and at the end of the main sequence. The grey lines correspond to our fit of the mass-radius relation of the seven short-period BH low-mass X-ray binaries.

However, this effect is not thought to be significant in LMXBs in quiescent state.

In order to calculate the evolution of the binaries, it is needed to know their mass-radius relation, since we need to know how the star responds to the loss of mass during mass transfer. For interacting binaries with white dwarfs accretors (cataclysmic variables, CVs), it has been shown that a power-law fit to the mass-radius relation $R_\star \propto M_\star^\alpha$ is an adequate description (Knigge et al. 2011).

We therefore model the mass radius relation of the companion stars in BH-LMXBs as $\frac{R_\star}{R_\odot} = f\left(\frac{M_\star}{M_\odot}\right)^\alpha$. We thus assume the BH-binaries to all align on the same slope in the logM-logR diagram. We fit the short-period binaries with a mass-radius index of ~ 0.82. We use this common power-law index as a fixed parameter to fit the mass-radius relation for each system, that is, for finding f for each binary. In Fig. 2 we show such a common power-law index with the grey lines, to be compared with the mass-radius relation of single MS stars (solid black lines). For comparison, the mass-radius relation for CVs has been fitted by Knigge et al. (2011) with $\alpha_{\rm CV} = 0.69$.

3.3 Kinematical properties and Galactic positions

The final (and crucial) piece of information we will use to reconstruct the birth of the BH is the position of the binary in the Galaxy. Assuming that the binary is born in the Galactic plane and receives a kick in the SN explosion right perpendicular to the plane, it will then move on a straight line reaching a maximum height $z_{\rm max}$. Assuming that the binary's current height z above the plane is $z_{\rm max}$, this height gives a minimum peculiar velocity at birth $v_{\perp,\rm min}$ given the Galactic potential at the distance R from the Galactic center (Paper I). The velocity $v_{\perp,\rm min}$ is the minimum velocity at birth required for bringing the system from the plane to its current position above (or below) the plane. This velocity is calculated simply by conserving the energy along the trajectory in the Galactic potential:

$$v_{\perp,\rm min} = \sqrt{2[\Phi\left(R_0, z\right) - \Phi\left(R_0, 0\right)]},$$

where $\Phi\left(R, z\right)$ is a model for the Galactic potential (Paczynski 1990) and R_0 is the observed projected distance of the binary from the Galactic centre.

In Table 2 we show the resulting values for $v_{\perp,\rm min}$ for our

Table 2. Kinematical properties of short-period black-hole low-mass X-ray binaries. The first group contains the binaries of this study. The second group contains the putative black hole candidates.

Source	distance [kpc]	z [kpc]	$v_{\perp,\rm min}$ [km/s]	Ref.
XTE J1118+480	1.62-1.82	1.43-1.61	70-75	[1]
GRO J0422+32	2.19-2.79	-[0.45-0.57]	25-30	[2]
GRS 1009-45	3.55-4.09	0.58-0.66	39-43	[3]
1A 0620-00	0.94-1.18	-[0.11-0.13]	9-11	[4]
GS 2000+251	2-3.4	-[0.10-0.18]	11-19	[5]
Nova Mus 91	5.63-6.15	-[0.69-0.76]	50-53	[6]
H 1705-250	6.5-10.7	1.02-1.68	361-441	[7]
MAXI J1305-704	2-8	-[0.26-1.06]	29-78	[8]
Swift J1357.2-0933	0.56.3	[0.38-4.83]	91-214	[9]
XTE J1650-500	1.9-3.3	-[0.11-0.20]	16-26	[10]
MAXI J1659-152	4.9-12.3	[1.39-3.50]	79-217	[11]
GRS 1716-249	2-2.8	[0.24 -0.34]	32-42	[12]
Swift J174510.8-262411	2-8	[0.05-0.19]	12-44	[8]
Swift J1753.5-0127	2-8	[0.42-1.69]	66-161	[8]
H 1755-338	4-9	-[0.34-0.77]	96-174	[13]
MAXI J1836-194	4-10	-[0.37-0.93]	39-112	[14]
XTE J1859+226	11-14	[1.65-2.09]	56-94	[15]
4U 1957+115	2-8	-[0.32-1.30]	36-94	[8]

References: [1] Gelino et al. (2006), [2] Gelino & Harrison (2003), [3] Gelino (2001), [4] Cantrell et al. (2010), [5] Barret et al. (1996), [6] Hynes (2005), [7] Remillard et al. (1996), [8] No acceptable estimates for the distance is available, so a distance of 5 ± 3 is assumed as done by Tetarenko, B.E. et al. 2015, in prep., [9] Shahbaz et al. (2013), [10] Homan et al. (2006), [11] Kuulkers et al. (2013), [12] della Valle et al. (1994), [13] Mason et al. (1985), [14] Russell et al. (2014), [15] Corral-Santana et al. (2011).

seven systems, as well as for the tentative BH candidates from Tetarenko, B.E. et al. 2015 (in prep). These BHs do not have a dynamical BH-mass estimate, but are likely BHs due to their spectral and timing properties (Tetarenko, B.E., priv. comm.). Of the sources contained in Tetarenko et al. catalogue, we select only the short-period ones. We show the range of possible values of $v_{\perp,\rm min}$ for every source in Fig. 3. It is interesting to note that there are 5 other sources whose minimum $v_\perp$ is very similar to the one of XTE J1118+480, which is one of the sources in our sample consistent with a high NK (see Sec. 6). Kuulkers et al. (2013) noted the similarities between XTE J1118+480, MAXI J1659-152 and Swift J1753.5-0127, pointing out their similar orbital period (few hrs) and the large scale height from the Galactic plane, suggesting that all three were kicked out of the Galactic plane, or possibly born in a GC (see also Shahbaz et al. 2013). We will suggest a similar interpretation for the remaining high peculiar velocity sources.

An estimate of the actual (rather than minimal) peculiar velocity received at birth can be obtained if the current 3D space velocity of the binary is measured. Integrating the trajectory of the binary backwards in time from the current initial conditions of the position and 3-D velocity, it is possible to infer the 3-D velocity at birth. The only system in our sample with measured both radial velocity and proper motion, and hence 3-D space velocity, is XTE J1118+480 (Miller-Jones 2014). Its Galactic trajectory has been integrated backwards by Fragos et al. (2009), giving a peculiar velocity at birth of $110 - 240$ km/s, which is consistent with our lower limit $v_{\perp,\rm min} \sim 70$ km/s.

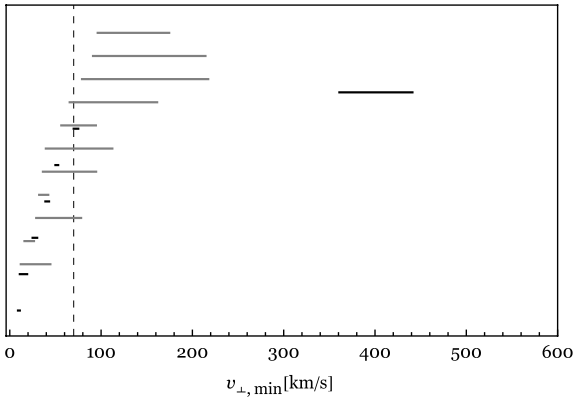

Figure 3. Range of possible values for the minimum peculiar velocity at birth of the short-period black hole X-ray binaries from Table 2. The solid lines indicate the systems belonging to our study. The grey lines indicate the BH candidates from Tetarenko, B.E. et al. 2015, in prep. The dashed vertical line indicates the lower limit on the peculiar velocity at birth for XTE J1118+480.

4 A semi-analytical method to follow the evolution of short-period BH-LMXBs

In order to link the observed properties of BH-LMXBs with BH formation, we will have to take the evolution of the binary since the BH formation into account. We use a semi-analytical approach to simulate the evolution of each binary in our sample. We follow the evolution of the three stages the binary goes through (BH formation, detached phase, mass transfer), but in reverse order.

Tracing backwards in time the mass transfer phase, we obtain the orbital properties of the binary at the onset of the Roche Lobe Overflow (RLO), $a_{\rm RLO}, M_{\star,\rm RLO}, M_{\rm BH,RLO}$, where $a_{\rm RLO}$ is the orbital separation. These properties will be a function of the mass transferred to the BH and of the mass-radius relation of the companion, both parameters that we vary. We then use these to calculate the orbital evolution due to the coupled effect of tides and magnetic braking during the detached phases following the BH formation. This then defines a set of potential progenitor binaries and BH formation properties (NK and mass ejection) that are consistent with the currently observed properties of BH-LMXBs.

4.1 Mass Transfer

The evolution of long-period BH binaries is driven by the nuclear expansion of the donor. Assuming the orbital angular momentum is conserved, one can trace the mass-transfer backwards in terms of the mass transferred to the BH (see Miller-Jones et al. 2009). We use a similar approach for dealing with the mass-transfer in short-period binaries, modeling it in an analytical way.

During Roche Lobe Overflow, the BH companion loses mass and its radius shrinks accordingly. Assuming that some type of orbital angular momentum loss always ensures the star is filling its Roche lobe, the shrinkage of the star induces a consequent shrinkage of the orbit. How much the orbit shrinks depends on the mass-radius relation $R_\star \sim M_\star^\alpha$ of the star. A similar approach was used for following the evolution of CVs by Knigge et al. (2011).

The rate at which the logarithm of the orbital separation a changes due to the combined effect of mass transfer, mass and angular momentum loss from the binary, is given by the following

balance equation:

$$\frac{\dot{a}}{a} = 2\frac{\dot{J}_{\rm orb}}{J_{\rm orb}} - 2\frac{\dot{M}_{\rm BH}}{M_{\rm BH}} - 2\frac{\dot{M}_\star}{M_\star} + \frac{\dot{M}}{M}, \quad (1)$$

where M is the total mass of the binary and $J_{\rm orb}$ the orbital angular momentum. We reparametrize the balance equation 1 in terms of $M_\star$, eliminating time as a variable. Solving the corresponding equation, we obtain the orbital separation a and mass of the BH at any point in the past, as a function of $M_\star$ and α, when the mass transfer is conservative (i.e. $\dot{M}_{\rm BH} = -\dot{M}_\star$). When the mass transfer is non conservative, an additional parameter is β ($\dot{M}_{\rm BH} = -\beta\dot{M}_\star$), and we assume that the matter leaves the binary with the specific angular momentum of the BH. The resulting analytic formulae are

$$\frac{a}{a_{\rm cur}} = \left(\frac{M_\star}{M_{\star,\rm cur}}\right)^{-\frac{1}{3}+\alpha}, \quad (2)$$

for conservative mass transfer, and

$$\frac{a}{a_{\rm cur}} = \left(\frac{M_{\rm BH}}{M_{\rm BH,cur}}\right)^{2-\frac{2}{\beta}} \left(\frac{M_\star}{M_{\star,\rm cur}}\right)^{-\frac{1}{3}+\alpha} \left(\frac{M}{M_{\rm cur}}\right)^{-\frac{8}{3}}, \quad (3)$$

for non-conservative mass transfer. The cur-subscript indicates values at the current time.

The mass transfer is traced backwards in this way until the onset of mass transfer. In order to define this, we have to assume how much mass is transferred since the onset, ΔM, and this defines $M_{\star,\rm RLO} = M_{\star,\rm cur} + \Delta M$. In our standard model we assume $\Delta M = 1\ M_\odot$. We will vary our assumptions on the mass transfer, namely the amount of transferred mass and the mass-radius index, when performing our simulations in Section 5. A smaller transferred mass and/or a smaller mass-radius index, will make the orbital separation at the onset of RLO smaller.

4.2 Detached evolution and BH formation

4.2.1 Coupling between tides and magnetic braking

To calculate the evolution during the detached phase preceding the mass transfer, we need to model the evolution of a system in which both tides and magnetic braking operate. Magnetic braking is the loss of angular momentum in a magnetic stellar wind (see Parker 1958, Weber & Davis 1967, Verbunt & Zwaan 1981). We refer to Repetto & Nelemans (2014) for details on the numerical method used to take into account the coupling between tides and magnetic braking. In short, after BH formation, the tidal torque circularizes and synchronizes the binary. From here, every bit of angular momentum lost from the star in its magnetic wind is also lost from the orbit, effectively shrinking the binary until the onset of RLO.

Our test-bed MB prescription was introduced by Verbunt & Zwaan (1981), and it gives the rate at which the star spins down $\dot{\omega}_\star$. This in turn gives the MB timescale, $\tau_{\rm MB} = J_{\rm orb}/\dot{J}_\star = J_{\rm orb}/I_\star\dot{\omega}_\star$, where $I_\star = k^2 M_\star R_\star^2$ is the moment of inertia of the star. Assuming the star is synchronized with the orbit ($\omega_\star = \omega_{\rm orb}$), one gets:

$$\tau_{\rm MB} = \frac{M_{\rm BH}}{M^2}\frac{1}{G\gamma_{\rm MB}k^2}\frac{a^5}{R_\star^4}, \quad (4)$$

where k is the gyration radius of the star and $\gamma_{\rm MB}$ is measured as $\approx 5\times10^{-29}{\rm s/cm}^2$.

For each of the seven binaries, we compute $a_{\rm max}$ such that RLO happens within the MS lifetime of the BH companion. The maximal orbital separation $a_{\rm max}$ is a function of the eccentricity of the binary right after the BH formation, and it depends on the MB calibration. The value of $a_{\rm max}$ varies only very little when taking a different calibration factor for tides, as shown in Repetto & Nelemans (2014).

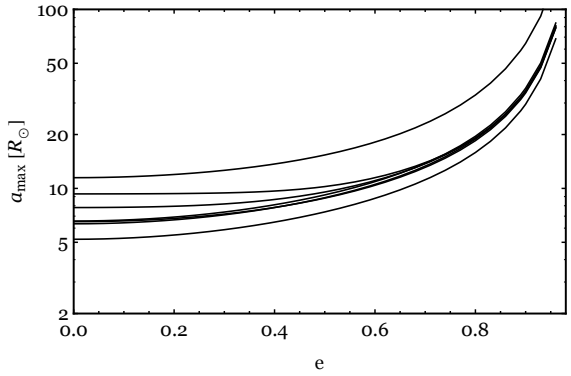

Figure 4. Maximal orbital separation right after black hole formation so that the star in short-period black-hole low-mass X-ray binaries fills its Roche Lobe within the main-sequence lifetime. From bottom to top, the curves are associated to the following sources: GRO J0422+32, 1A 0620-00 and Nova Mus 91 (overlapping curves), GRS 1009-45, GS 2000+251, H 1705-250, XTE J1118+480.

We numerically fit $a_{\rm max}$ as a function of the eccentricity e and of the orbital separation at the onset of RLO, $a_{\rm RLO}$:

$$a_{\rm max}(e, a_{\rm RLO}) = \alpha + \beta(1-\exp(\gamma e)) + \frac{\delta e}{e-\epsilon} \quad (5)$$

where $\alpha, \beta, \gamma, \delta, \epsilon$ are the parameters of the fit, and they depend on $a_{\rm RLO}$ (see Appendix B).

We test two types of magnetic braking law: one from Verbunt & Zwaan (1981) (VZ, hereafter), and the other one from Ivanova & Taam (2003) (IT, hereafter). The tidal model is based on Hut (1981) and we use calibration factors as in Hurley et al. (2002).

We show $a_{\rm max}$ as a function of the eccentricity in Fig. 4 for the seven sources we are studying, when using a VZ-type of magnetic braking. The orbital separation of the RLO configuration $a_{\rm RLO}$ is computed using formula 2, tracing the mass transfer phase backwards in time from the current properties, until the companion-star mass increases to $1\ M_\odot$.

We wish to note that the orbital separation $a_{\rm max}$ is not affected by the rate at which the companion star is initially spinning. This is due to the fact that the angular momentum stored in the star is much less than the angular momentum stored in the orbit. The ratio between the value of $a_{\rm max}$ when taking a star initially spinning at $\omega_\star \approx 0.9\ \omega_{\rm break}$ and the value when the stellar spin is $\omega_\star \approx 10^{-6}\ {\rm s}^{-1}$, is between $1-1.5$ for every value of the eccentricity.

Another way of computing $a_{\rm max}$ is simply by requiring that $\tau_{\rm MB} \leqslant \tau_{\rm MS}$, as done for instance by Kalogera (1999). The orbital separation used for computing $\tau_{\rm MB}$ is the circularized orbital separation after BH formation. As an example, in the case of the binary XTE J1118+480, $a_{\rm max}$ computed using timescale considerations differs only little from $a_{\rm max}$ in our model, by 15% at most.

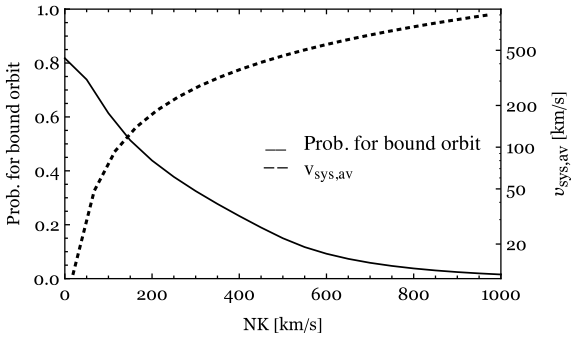

Figure 5. Probability for a binary containing a black hole of mass 8 $M_\odot$ and a companion with mass 1 $M_\odot$ of having survived the supernova event (solid line) as a function of the natal kick. The dashed line shows the averaged systemic velocity acquired by the binary in the supernova event.

4.3 Supernova dynamics

The orbital configuration right after BH formation ‡ can be determined univocally from the properties of the pre-BH-formation configuration through conservation of orbital energy and orbital angular momentum. An abundance of earlier studies deal with the effect of a SN explosion and possibly of a NK on the orbital configuration (see for example Blaauw 1961, Boersma 1961, Hills 1983, Kalogera 1996). In this way, one can compute the orbital elements $a_{\rm post}, e_{\rm post}$ knowing $a_{\rm pre}, e_{\rm pre}$, the magnitude and direction of the NK, and the amount of mass ejected from the collapsing star (mass which is assumed to leave the system instantaneously without further interacting with the binary). The effect of the NK and the mass ejected at BH formation combine together to give the total peculiar (also called *systemic*) velocity of the binary:

$$V_{\rm pec} = \sqrt{\left(\frac{M_{\rm BH}}{M'}\right)^2 V_{\rm NK}^2 + V_{\rm MLK}^2 - 2\frac{M_{\rm BH}}{M'} V_{\rm NK,x} V_{\rm MLK}}, \quad (6)$$

where M' is the total mass after the binary has lost a mass $M_{\rm ej}$ in the SN, $V_{\rm NK}$ is the magnitude of the NK, $V_{\rm NK,x}$ its component along the orbital speed of the BH progenitor, and $V_{\rm MLK}$ is the *mass-loss kick*, the recoil the binary gets after a mass $M_{\rm ej}$ is lost, also known as *Blaauw kick* (Blaauw 1961):

$$V_{\rm MLK} = \frac{M_{\rm ej}}{M'}\frac{M_\star}{M}\sqrt{\frac{GM}{a}}, \quad (7)$$

where M is the total mass of the binary right before the SN.

In Fig. 5, we show the probability for the binary to stay bound in the SN event (solid line). This probability is calculated for a sample of binaries formed by a BH of mass 8 $M_\odot$ and a companion of mass 1 $M_\odot$, with randomized initial orbital separations and ejected mass, and random orientation of the NK. The probability is calculated as a function of the NK. We also show (dashed line) the average systemic velocity acquired by the binary in case it stays bound.

4.4 Monte Carlo calculation of BH formation and detached evolution

Once we have the properties at RLO, we treat the BH formation phase with a Monte Carlo approach. We build a sample of 80×10^6 initial binaries formed by a companion of mass $M_{\star,\rm RLO}$ and the progenitor of the BH with mass $M_{\rm prog} = M_{\rm BH,RLO} + M_{\rm ej}$, where $M_{\rm ej}$ is drawn from a uniform distribution between 0 and 10 $M_\odot$. The orbital separation of the initial binary is drawn from a uniform distribution between a minimum value and 50 $R_\odot$, and the orbit is assumed to be synchronous and circular. The minimum value for the orbital separation is the value at which the Helium star and/or the companion overfill their Roche lobe. The Helium star ejects a mass equal to $M_{\rm ej}$, and what is left collapses into a BH, which receives a NK at formation drawn from a uniform distribution between 0 and 1000 km/s. The inclination of the NK with respect to the orbital plane is uniformly peaked over a sphere centered on the progenitor of the BH.

The motivation which lays behind our choice of the range for the initial orbital separation is statistics. Orbital separations larger than 50 $R_\odot$ will only very rarely lead to RLO within the MS lifetime. Specifically, RLO on the MS will happen only if the binary is highly eccentric in the post-SN configuration. This can be seen from the decaying PDFs at large values for the pre-SN orbital separation in Fig. 13. We tested this assumption checking how many systems with initial orbital separation $a_{\rm pre} > 50\ R_\odot$ evolve into successful ones. For all sources except XTE J1118+480, no simulated binary with $a_{\rm pre} > 50\ R_\odot$ evolves into a successful one. For XTE J1118+480 the fraction of systems which evolve into successful ones is 9%.

Concerning the NK and the $M_{\rm ej}$, those ranges are rather arbitrary, due to the great uncertainty on the BH formation process. Nevertheless, larger values for the NK and for the $M_{\rm ej}$ than the extreme ones we chose, would lead to an unbinding of the system, hence they are of no interest to our work.

Using the formalism we showed in Section 4.3, we compute $a_{\rm post}$ and $e_{\rm post}$. We assume that the SN ejecta do not have any impact on the companion star properties, its spin for instance, hence $\omega_{\star,\rm post} = \omega_{\star,\rm pre} = \omega_{\rm orb,pre}$. To account for the coupling between tides and magnetic braking, we make sure that $a_{\rm post}$ is less than the value of the maximal orbital separation at that eccentricity and at the calculated $a_{\rm RLO}$ (Section 4.2.1). An additional criterion which allows to constrain the allowed parameter space of NK and $M_{\rm ej}$ is the kinematical one: we make sure that the peculiar velocity acquired by the binary at BH formation is larger than the minimum peculiar velocity $v_{\perp,\rm min}$ we inferred from the position of the binary (see Section 3.3).

4.5 Observational biases on our sample

4.5.1 Results from the population model

Because we want to derive general conclusions on the NK and ejected mass at BH formation, we want to generalize the results for the individual systems. In order to do so, we want to have some idea of the effect of the different NKs and ejected masses on the observational properties of the systems, and thus of possible observational biases that make that the observed systems are predominantly those with particular NKs and/or ejected masses.

We build a population of BH-LMXBs formed by a BH of mass 8 $M_\odot$ and a companion of mass 1 $M_\odot$. The magnitude of the NK, the mass ejected at BH formation, and the initial orbital separation are drawn from uniform distributions between 0 - 1000 km/s, 0 - 10 $M_\odot$, and 0 - 50 $R_\odot$ respectively, whereas the orientation of the NK is random over a sphere centered on the BH progenitor. For those binaries that stay bound in the SN, we select only those ones which undergo RLO within the MS lifetime. We show the re-

‡ Throughout the whole paper, we denote with *-pre* the binary configuration right before the BH formation, with *-post* the configuration right after.

sults in Fig. 6. The higher density region is for mild kicks around $100 - 200$ km/s, and small $M_{\rm ej}$. Such a combination of these two parameters, allow the orbital separation in the post-SN configuration to fall within $a_{\rm max}$.

We then populate the Galaxy following the stellar density in the thin disc (Binney & Tremaine 2008 and McMillan 2011), and we follow the trajectories of the successful binaries for 10 Gyr. The observed BH low-mass X-ray binaries all lie within 10 kpc from the Sun (see Table 2). This is very likely due to the fact that the binary has to be relatively close so that a dynamical measurement of the BH mass via optical spectroscopy is possible. We analyze how many of the simulated binaries satisfy this proximity-criterium as a function of the NK and $M_{\rm ej}$. We show the results of this calculation in Fig. 7, where for every bin (NK, $M_{\rm ej}$) of the plot in Fig. 6, we compute the fraction of systems that lie within 10 kpc from the Sun with respect to the total number of winning binaries in that bin. From the plot, it is evident that we are biased towards binaries in which the BH received a low NK. So even if BHs received high kicks, we would not observe most of them.

4.5.2 *Hyper-velocity systems*

Related to the previous discussion, we wonder how likely it is that we are missing systems in the halo of the Galaxy. Taking a Galactic local escape velocity of $\sim$ 500 km/s (Smith et al. 2007), the minimum NK the BH has to acquire for the binary to escape the Galactic potential, is $\sim$ 550 km/s (for every choice of initial orbital separation and ejected mass in the SN). A binary moving with a peculiar velocity of 500 km/s would travel a distance of 500 kpc in 1 Gyr. However, the probability for the binary to stay bound with such a large NK is of ≈ 0.1 only, as we can see in Fig. 5. Thus, we expect most of these hyper-velocity binaries to get unbound.

Yet, it is likely that we are missing systems in the halo of our Galaxy. We performed a test integrating the Galactic orbit of BH-LMXBs in which the BH received a NK at birth. Even with a mild NK of 200 km/s, the BH-LMXB would move far away from the Sun reaching the halo in 10 Gyr, out to $R \sim 60$ kpc. So even if the binary stays bound in the BH formation event, it would remain undetectable optically.

5 Results

With the numerical method described above we calculate the possible combinations of NK and ejected mass that are compatible with the observed properties of the seven BH-LMXBs in our sample.

5.1 Different models

We vary the physics involved in the binary evolution (mass-radius power-law index α, maximum transferred mass ΔM) and we take into account the uncertainty in the distance of the source, to test what is the resulting uncertainty on the lower limits for the NK and the mass ejected in the SN. Furthermore, we test the different MB prescriptions (VZ and IT, see Section 4.2.1). The models we test are:

(i) (standard model) VZ, $\Delta M = 1 M_\odot, \alpha = 0.82$
(ii) IT, $\Delta M = 1 M_\odot, \alpha = 0.82$
(iii) VZ, $\Delta M = 0.4 M_\odot, \alpha = 0.82$
(iv) IT, $\Delta M = 0.4 M_\odot, \alpha = 0.82$
(v) VZ, $\Delta M = 1 M_\odot, \alpha = 0.69$

For all the models, we simulate 80×10^6 initial binaries.

5.2 Lower limits on the natal kick and ejected mass

We show in Fig. 8 the density plots of possible combinations of NK-$M_{\rm ej}$ that can lead to the currently observed properties of the seven systems, for Model (i).

There is a typical trend in the higher-density region of the plots, which indicates an increasing ejected mass for an increasing natal kick. This is caused by the constraint on the orbital separation in the post BH-formation configuration: the binary has to be compact enough for mass transfer to start while the companion is still on the MS. In the absence of a large NK, large ejected mass would widen the system too much. Only if a NK counters that effect are larger ejected masses permitted; but there is a decreasing fraction of NK-orientations that allow this (see the decreasing density along the trend).

The density plots clearly separate the systems in at least two classes: five systems that have the highest densities at or close to the origin, and two systems (H1705-25 and XTE J1118+480) that have the highest densities at large NK. However, there is still a significant difference between the five low-kick systems: two of them (Nova Mus 91 and GRS 1009-45) actually exclude or have very low density to have no kick. Finally, we note that all systems have significant density at $M_{\rm ej} = 0$.

We need to point out that these distributions do not correspond to probability distributions of the actual values of the parameters for the systems, as the parameter range and parameter distributions that we used in the Monte Carlo (flat) will likely not represent the real ones. However, as we used flat input distributions, the resulting probabilities do show how much fine tuning in the initial binary parameters and NK orientations is needed to survive and match the kinematic and orbital properties of the binaries.

In order to quantify our results, we show in Fig. 9 and 10 the cumulative distribution for the NK and for the ejected mass for each of the 7 sources for our Monte Carlo calculations. We define a *minimum* NK and ejected mass as a cut at the 5% probability in these cumulative distributions, i.e. a limit at which the 95% of the cumulative distribution is higher. These lower limits are shown in Table 3 and the range of values for each of the sources is a consequence of the uncertainty on the physics involved (i.e. the different models we use) and on the distance. The variation of the parameters involved in the binary evolution, namely the amount of mass transferred to the BH, the mass-radius index and the strength of MB, do not affect greatly the lower limits on the NK and on the $M_{\rm ej}$ (see second and third column in Table 3 for the first six binaries). These lower limits are mostly affected by the peculiar velocity of the system, hence by the height of the system from the Galactic plane, and are therefore consistent with the ones by Repetto et al. (2012) that accounted for the kinematics of the sources only. Indeed, in the case of H 1705-250, the large range for the NK is due to the large (25%) uncertainty in the distance to the source. Whereas the large value for the NK is due to the fact that the binary resides right above the Galactic bulge, very close to the Galactic centre where the Galactic potential is strongest.

Typically, these lower limits fall in lower density regions of the plots in Fig. 8 and thus still require severe fine tuning of in particular the NK orientation. We also wish to note that assuming all (x, y, z) directions for the NK are equally probable, the lower

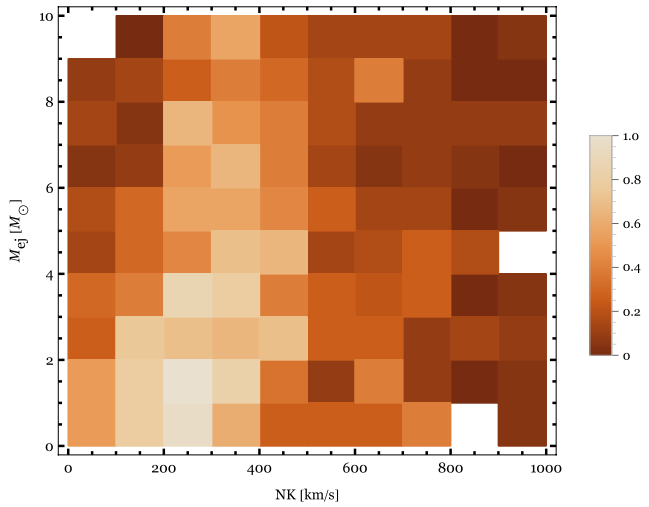

Figure 6. Results of a binary population synthesis study of black-hole LMXBs. We select only those binaries which undergo RLO within the MS lifetime, and we show their optimal parameter space for the mass ejected in the SN and the NK.

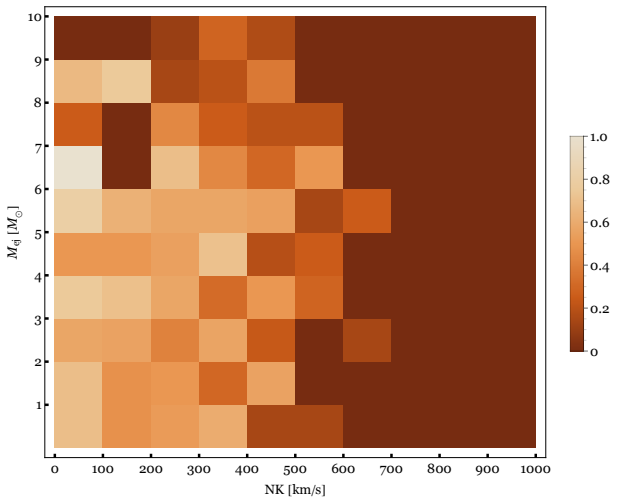

Figure 7. For every 2D-bin of the left plot, we show here the fraction of systems which reside within 10 kpc from the Sun after orbiting in the Galactic potential for 10 Gyr.

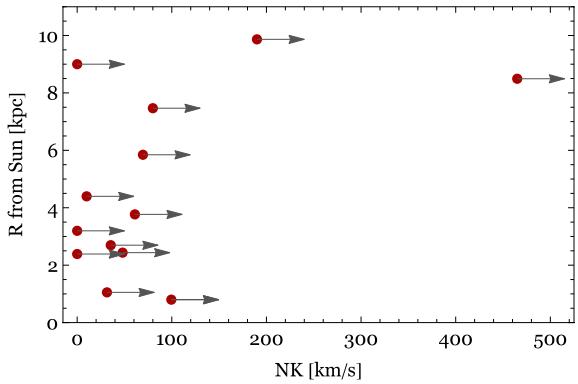

Figure 11. BH low-mass X-ray binaries as a function of their distance R from the Sun and the lower limit on the NK, as computed in Paper I and in this work.

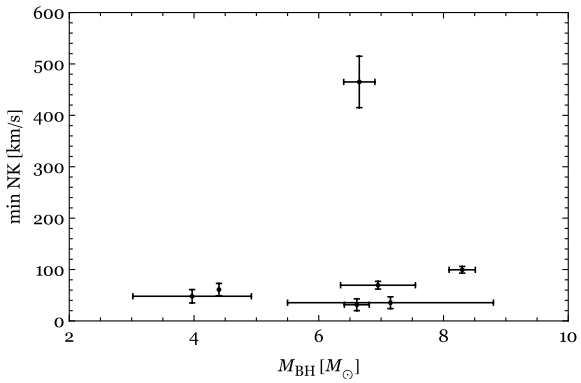

Figure 12. Short-period BH low-mass X-ray binaries as a function of black hole mass and the minimum natal kick which results from our simulations.

limits for the NK indicated in the table are to be multiplied by the square root of 3.

We also checked the effect of taking a non-conservative mass transfer rather than a conservative one, using formula 3 for tracing backwards the semi-detached phase, and taking $\beta = 0.1$. When comparing the results of this model with the results of Model (i), for example, we find that the lower limits on the NK and on M_{ej} do not change by more than 7%, for all the 7 sources.

The fact that all the highest-density regions in Fig. 8 are skewed towards low kicks (except for H 1705-250 and XTE J1118+480), does not mean that high BH kicks are excluded. The reason why we are biased towards small NKs is the proximity of the sources to the Sun. This can be seen in Fig. 11, where we plot the whole sample of confirmed BH low-mass X-ray binaries as a function of their distance to the Sun and the lower limit on the NK. Referring back to our BPS study, it is evident that the higher the kick, the lower the probability for the system to be in the proximity of the Sun (see Fig. 7).

From our results, it is possible to highlight three different cases:

(i) *Standard systems*: systems with a low peculiar velocity at birth, which can be consistent either with a small NK, or with a kick imparted to the binary as a result of the mass ejection in the SN event.

(ii) *Zero ejected mass systems*: systems consistent with a non-zero NK *but* zero ejected mass at BH formation.

(iii) *High NK systems*: systems consistent with a high NK, comparable to NS natal kicks.

We will discuss these three scenarios in Sec. 6.

5.3 Correlation natal kick VS mass of the BH

In Fig. 12 we plot our lower limits for the NK as a function of the BH mass to see if there is any correlation. From our results, we find so far (with our limited sample) no evidence for a correlation between NK and BH mass. If we found a correlation, such as lighter BHs receiving higher kicks, that could be a hint for a NK happening on a shorter timescale than the fallback timescale.

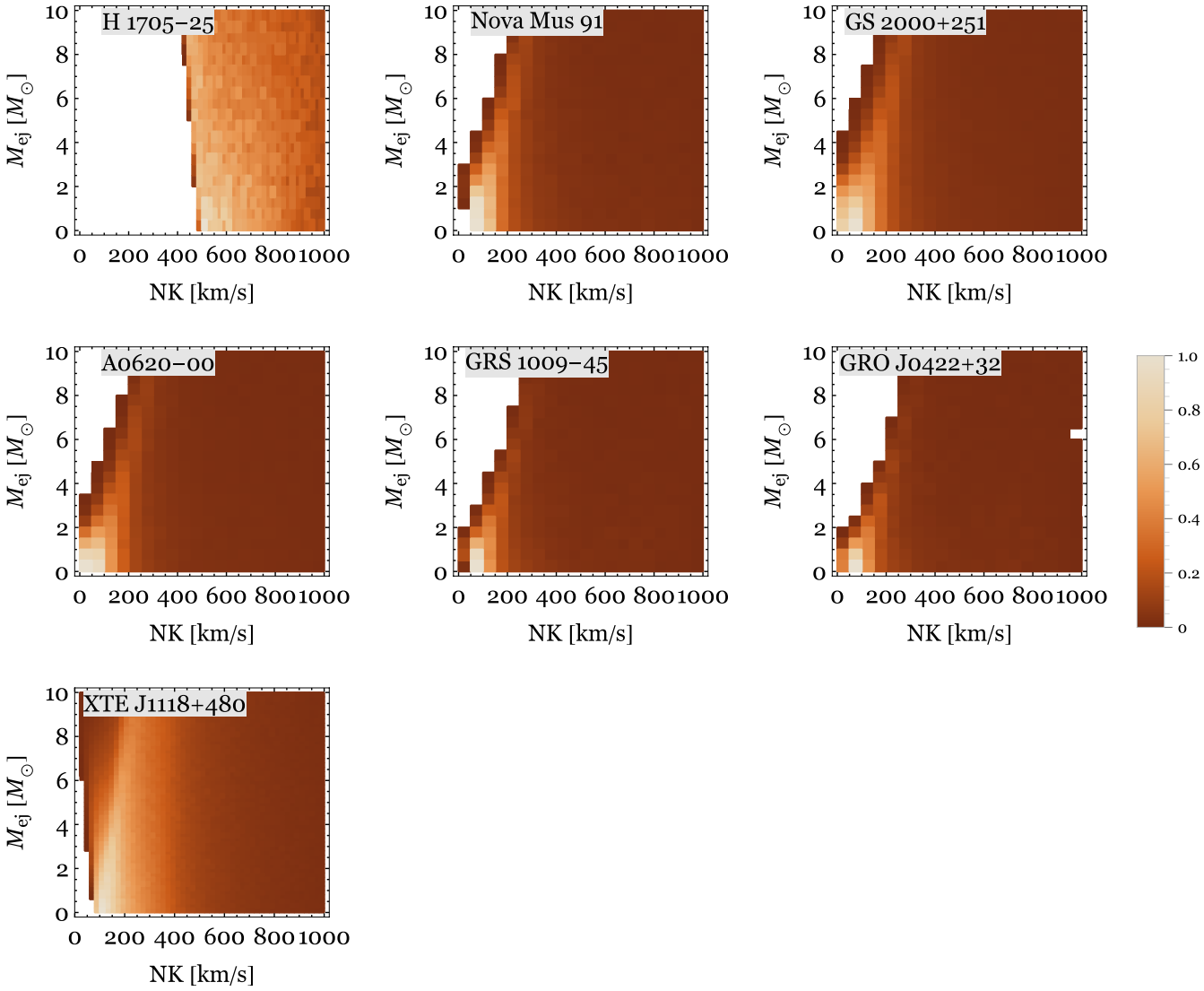

Figure 8. Density plots showing the allowed parameter space for the mass ejected M_{ej} and the natal kick NK at BH formation for the seven short-period black-hole low-mass X-ray binaries, in the framework of our standard model (i), see text for details.

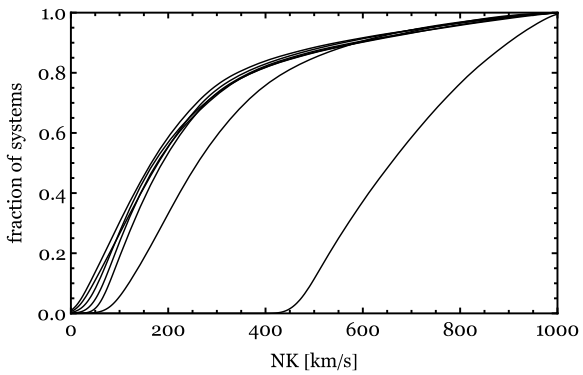

Figure 9. Cumulative distribution for the natal kick received by the black hole in short-period BH-LMXBs, in the framework of our standard model (i), see Text for details. From left to right: 1A 0620-00, GS 2000+251, GRO J0422+32, GRS 1009-45, Nova Mus 1991, XTE J1118+480, H 1705-250.

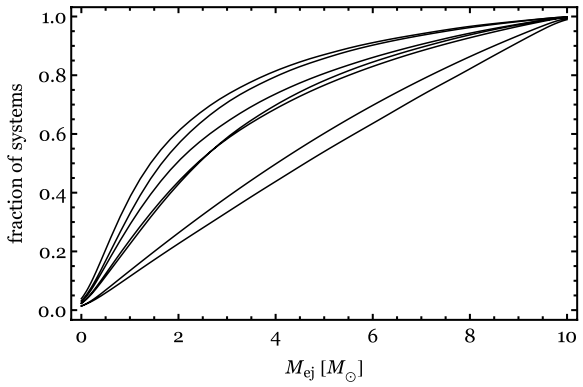

Figure 10. Cumulative distribution for the ejected mass at BH formation in short-period BH-LMXBs, in the framework of our standard model (i), see Text for details. From left to right: GRO J0422+32, 1A 0620-00, GRS 1009-45 and Nova Mus 1991 (overlapping curves), GS 2000+251, XTE J1118+480, H 1705-250.

Table 3. The second and third column show the minimum natal kick and the minimum mass ejected at BH formation. The third column shows $a_{\rm pre,max}$ such that the binary undergoes mass transfer within the MS lifetime. The range indicates how the values vary when changing the assumption on the parameters involved in the binary evolution of the sources (see Text for a description of the different models we consider). The last column shows $a_{\rm pre,max}$ such that the binary stays bound in the SN.

Source	min NK [km/s]	min $M_{\rm ej}$ [$M_\odot$]	max $a_{\rm pre}$, RLO on MS [$R_\odot$]	max $a_{\rm pre}$, bound in SN [$R_\odot$]
GS 2000+251	24-47	0.13-0.33	9-37	7800
A0620-00	20-43	0.09-0.32	8-37	8400
Nova Mus 91	62-77	0.17-0.34	8	1400
XTE J1118+480	93-106	0.31-0.37	23-38	570
GRS 1009-45	49-73	0.08-0.28	8-38	2400
GRO J0422+32	35-61	0.04-0.26	7-38	3000
H 1705-250	415-515	0.40-0.50	11-19	27

5.4 Initial orbital separation

We show in Fig. 13 the probability density function for the orbital separation right before BH formation for the seven sources.

In the third column of Table 3, we show the maximal orbital separation right before BH formation such that the binary stays bound in the SN *and* undergoes mass transfer within the MS-lifetime. In the fourth column, we show the maximum value for $a_{\rm pre}$ such that the binary stays bound in the SN. The range of values correspond to varying our models. Comparing the values of the last two columns, we see that the constraint to have RLO within MS lifetime, is much more limiting than having the binary to stay bound in the SN. As a consequence, we expect that there are many detached BH+MS-star binaries which would evolve to longer and longer periods due to the nuclear expansion of the companion, finally evolving into BH+WD binaries.

6 Discussion

There are three BH-formation scenarios which are compatible with some of the seven sources we studied.

6.1 Zero ejected mass systems

Five systems (H 1705-250, Nova Mus 91, GRS 1009-45, GRO J0422+32, XTE J1118+480) are consistent with a NK, while not requiring the ejection of mass at BH formation. The NK at which the one dimensional NK density function for $M_{\rm ej} = 0$ peaks is correspondingly: 525, 76, 68, 54, 114 km/s. We wish to stress that these value do not correspond to the most likely value of a probability density function, rather they are the values of the NK which require less fine-tuning.

Zero ejected mass at BH formation could be consistent with a BH formed in the dark (no SN, i.e. no baryonic mass ejected) and with a NK caused by asymmetric neutrino emission or asymmetric GW emission. When a BH is formed, the gravitational mass defect which is equal to the negative binding energy, is calculated to be $\sim 10\%$ of BH mass (Zeldovich & Novikov 1971). If this mass leaves the system in the form of neutrinos, the predicted ejected mass can be consistent with our limits of Table 3.

We note, however, that in the case of XTE J1118+480 there is evidence for an explosion having occurred from the chemical enrichment in the spectra of the companion to the BH (González Hernández et al. 2006).

Furthermore, we wish to highlight that our study is the first in suggesting that few of the BHs in LMXBs might have been formed without baryonic mass ejection. This was found for few BHs in high-mass X-ray binaries (see Valsecchi et al. 2010, Mirabel & Rodrigues 2003).

6.2 Standard systems

Five sources out of seven (Nova Mus 91, GS 2000+251, 1A 0620-00, GRS 1009-45, GRO J0422+32) require only a small peculiar velocity at birth, of the order of few tens of km/s or less (see Table 2). This small peculiar velocity could be imparted to the binary as a result of mass ejection in the SN event. We can compute how much ejected mass is needed to account for the small peculiar velocity (see Fig. 14), in a similar manner as done previously by Nelemans et al. (1999). In order to compute the kick received by the binary due to the mass ejection (MLK), we use formula 7. We trace the orbital binary properties backwards assuming a transferred mass of $1\ M_\odot$ and $\alpha = 0.82$. As a test, we assume a semi-major axis in the pre-SN configuration of $1.5\ a_{\rm RLO}$ (solid line) and of $5\ a_{\rm RLO}$ (dashed line). The plots show the amount of mass ejected needed to account for the peculiar velocity of the 5 sources aforementioned. There is an upper limit on $M_{\rm ej}$ such that the binary stays bound in the SN, i.e. the ejected mass has to be less than half of the total initial mass, which translates into $M_{\rm ej} < M_{\rm BH} + M_\star$ (vertical lines in Fig. 14). All of the five systems but Nova Mus 91, can be explained by mass-ejection only.

Alternatively, density wave scatterings could impart a velocity to the system of the order of few tens km/s (Brandt et al. 1995), with a maximum value of 40 km/s (Mihalas & Binney 1981).

As previously discussed in Sec. 3.1, GRS 1009-45 lacks strong constraints on the masses of its components. In particular, the BH mass quoted in Table 1 is a strict lower limit. We then estimate the MLK taking a larger BH mass of $7\ M_\odot$ and a companion mass of $0.98\ M_\odot$. We find that for $a_{\rm pre} = 1.5\ a_{\rm RLO}$, the ejected mass needed to account for the peculiar velocity of the system is $\sim 7\ M_\odot$. Calculations by Fryer & Kalogera (2001) indicate a maximum ejected mass at BH formation of $\sim 4\ M_\odot$. We conclude that it is essential to better constraint the component masses in GRS 1009-45 in order to discriminate between a standard scenario and a non-zero NK scenario.

Concerning GRO J0422+32, we check what is the effect of using BH and companion-star masses from Reynolds et al. (2007) ($M_{\rm BH} = 10.4\ M_\odot$ and $M_\star = 0.4\ M_\odot$). For $a_{\rm pre} = 1.5\ a_{\rm RLO}$, the MLK is always lower than the peculiar velocity of the systems, for every $M_{\rm ej}$. Again, this highlights the importance of correctly estimating the component masses.

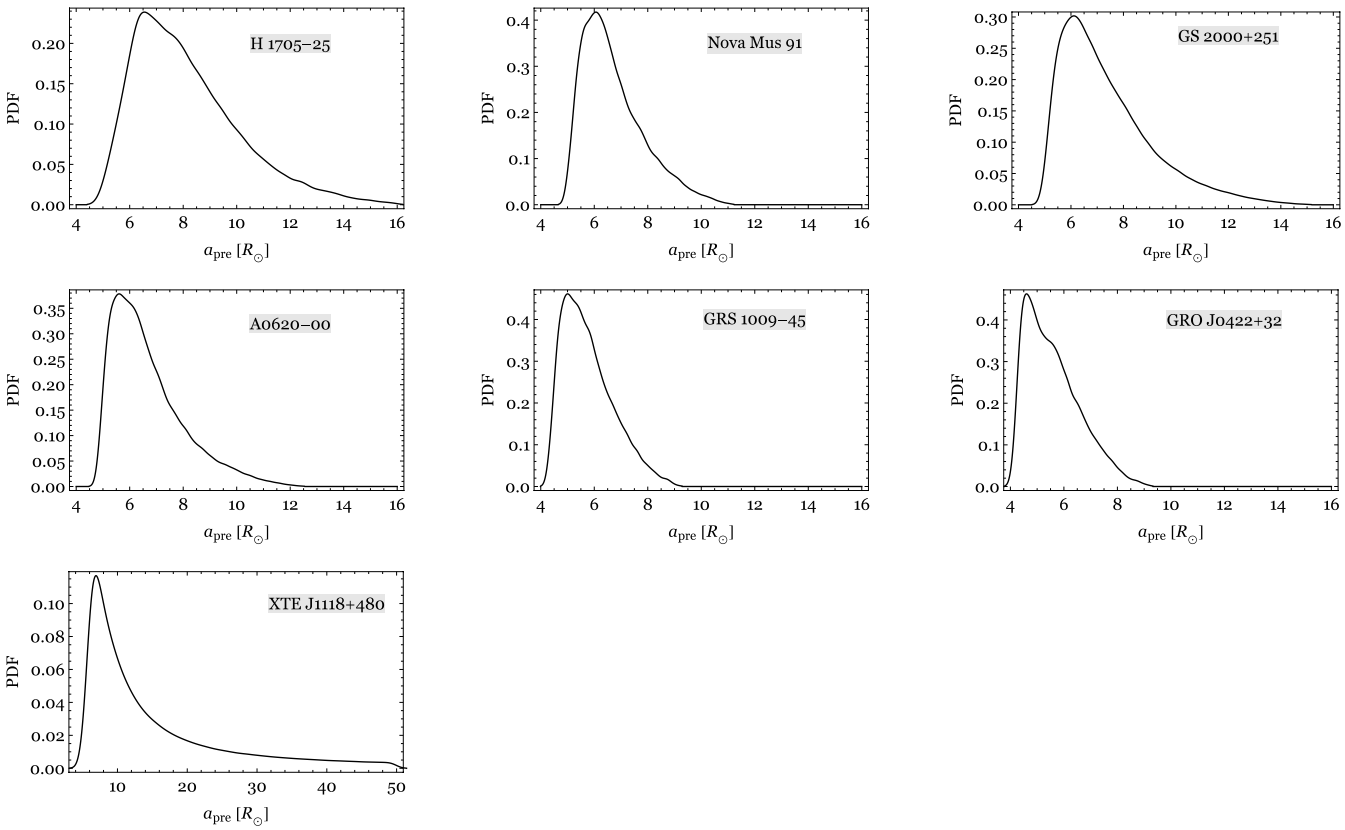

Figure 13. Probability density function for the orbital separation right before black hole formation for short-period BH-LMXBs, in the framework of our standard model (i), see Text for details.

6.3 High natal kick systems

Two out of seven sources require a high NK at birth (H 1705-250 and XTE J1118+480), comparable to NS natal kicks. This could be a hint for the NK happening on the same timescale of the fallback. A high NK for the BH in XTE J1118+480 was already suggested by Fragos et al. (2009).

As an alternative explanation, these two systems could have been ejected from a GC. None of the BH X-ray binaries currently known are found in a GC. So far, there is evidence for two BHs in a Milky Way GC (Strader et al. 2012), and one BH in an extragalactic GC (Maccarone et al. 2007). However, no optical companion has yet been found for these candidates, hence an accurate estimate of the mass of the compact object does not exist. A GC origin for XTE J1118+480 seems unlikely, due to the super-solar surface metallicity of the companion (Fragos et al. 2009, González Hernández et al. 2006).

H 1705-250 is the source which looks most different from all the other sources in the sample. It is located right above the Galactic bulge, at Galactic coordinates $R \sim 0.5$ kpc, $z \sim 1.35$ kpc. Its systemic radial velocity was measured by Remillard et al. (1996), giving a value of 10 ± 20 km/s. We conclude that either the system is moving perpendicularly to our line of sight, or that a GC origin for the system is more likely.

Looking at Fig. 3, there might be at least 5 other systems hinting for a high NK, those ones whose peculiar velocity at birth $v_{\perp,\rm min}$ is similar to the one of XTE J1118+480. Future work is needed to precisely determine the mass of the compact object in such systems.

6.4 Effect of the uncertainty on the distance

The most accurate method to determine the distance to a BH X-ray binary, is to estimate the absolute magnitude of the companion star, see Jonker & Nelemans (2004). This method has been used for all the 7 BH-LMXBs in our sample, except for Nova Mus 91, for which the distance was estimated by Hynes (2005) through the interstellar absorption properties of the source, which is a less reliable method. Orosz et al. (1996) found a distance of $d = 5.5 \pm 1$ kpc, estimating the spectral type and luminosity of the companion. Such a distance would give $v_{\perp,\rm min} = 50 - 56$ km/s, still consistent with our value of $v_{\perp,\rm min} = 50 - 53$ km/s (see Table 2).

The major source of systematic errors when estimating the distance through the absolute magnitude of the companion, comes from a failure in accounting for the right disc-contribution to the light of the star (see Sec. 6 in Paper I for a discussion). Hynes (2005) warn about possible systematics on the measurement by Gelino (2001) of the distance to GRS 1009-45, due to the assumed small veiling from the disc. Taking into account a larger contribution from the disc, Barret et al. (2000) obtained a distance $d = 5 - 6.5$ kpc. This translates into a minimum peculiar velocity $v_{\perp,\rm min} = 48 - 52$ km/s, larger than the one taken in our work (see Table 2). This results in a minimum NK of ~ 62 km/s, when performing a set of simulation in the framework of our standard model (i). This value is still consistent with the range shown in Table 3.

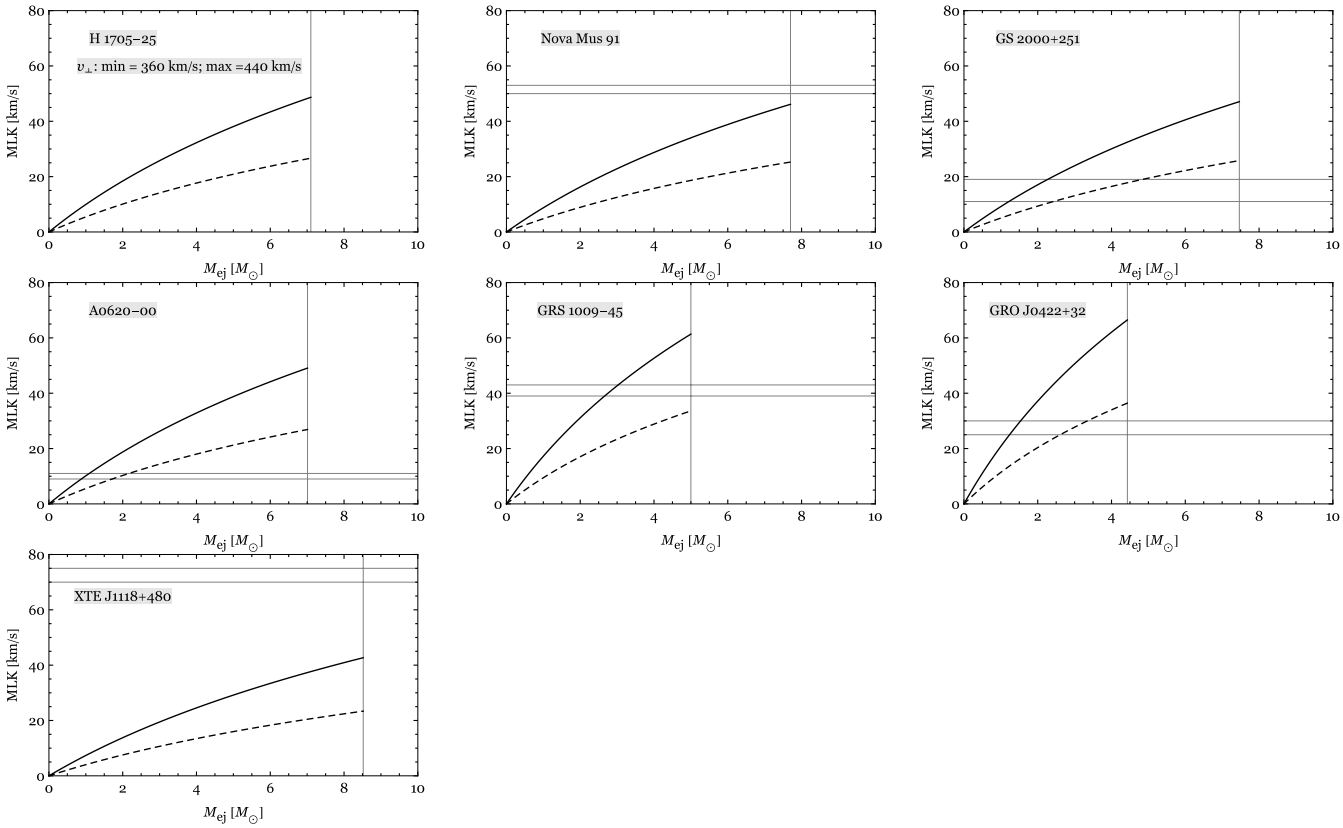

Figure 14. Mass-loss kick (MLK) as a function of the mass ejected at BH formation for the short-period BH-LMXBs. The vertical lines show the upper limit on the mass ejected at BH formation for the binary to stay bound. The solid gray lines correspond to the lower and upper limit on the peculiar velocity at birth. The black solid and black dashed line correspond to different assumptions on the pre-SN orbit (see Text). The point of intersection between these lines and the limits on the peculiar velocity depicts when a system can be explained by mass ejection only.

7 Conclusions

There are five main conclusions which result from this work:

(i) The lower limit on the NK is not greatly affected by the binary evolution of the sources. It is mostly affected by the kinematics of the system, and therefore by the uncertainty on the distance. In this respect, our results are consistent with the ones in Repetto et al. (2012), who calculated lower limits on BH natal kicks basing their study on kinematical arguments. Variations of the assumptions on MB and mass transfer give very similar results.

(ii) Even if the lower limit on the NK is not affected by the binary evolution of the system, in order to unravel what are the optimal combinations of NK and mass ejected in the SN, it is necessary to follow the details of the whole evolutionary paths of BH-LMXBs. In particular, this method allowed us to find binaries consistent with a neutrino-driven NK.

(iii) Our work enables us to highlight three possible scenarios for the birth of the BH. Two of these scenarios have been discussed previously in the literature: either the BH does not receive any NK, or it receives a NS-like NK. The third scenario that we suggest, is a BH having formed with a NK and zero baryonic mass ejection. It is the first time that this scenario has been applied to the evolution of BH-LMXBs, whereas it was first found to be consistent with the formation of few BHs in high mass X-ray binaries (see Valsecchi et al. 2010, Mirabel & Rodrigues 2003).

(iv) We find evidence for a high NK (i.e. a NS-like NK) in two of the sources, and potentially 5 BH X-ray binary candidates whose minimum peculiar velocity at birth suggests a high NK.

(v) Our population study highlights that, due to the limits of optical spectroscopy, there exists a bias towards BH-LMXBs being close (within 10 kpc) to the Sun. For the same reason, NK estimates are biased towards low/mild NKs (less than $100 - 200$ km/s).

8 Acknowledgments

We are grateful to the anonymous referee for very pertinent insights, especially on the observational properties of the binaries, and on the implications of the uncertainty on these properties on our study. SR thanks Bailey Tetarenko for having provided the catalogue of BH candidates, and for her thorough and critical reading of the manuscript. The work of SR is supported by the Netherlands Research School for Astronomy (NOVA).

A Analytical treatment of the mass transfer phase

The orbital angular momentum of a binary is written as

$$J_{\rm orb} = \mu\sqrt{GMa},$$

in terms of the reduced mass μ, the total mass of the binary M, and the semi-major axis a. Using Paczyński (1971) relation for the Roche radius, $R_L \approx 0.46\, a\, \left(\frac{M_\star}{M}\right)^{1/3}$, and the fact that the star is

filling its Roche lobe during mass-transfer, $R_L = R_\star = fM_\star^\alpha$, we can express $J_{\rm orb}$ in terms of the component masses only:

$$J_{\rm orb} = \sqrt{Gf} M_{\rm BH} M^{-1/3} M_\star^{\frac{5}{6}+\frac{\alpha}{2}}$$

This expression can then be derived with respect to $M_\star$:

$$\frac{dJ_{\rm orb}}{dM_\star} = M_{\rm BH} M^{-\frac{1}{3}} (\frac{5}{6}+\frac{\alpha}{2}) M_\star^{-\frac{1}{6}+\frac{\alpha}{2}} \sqrt{Gf} - M^{-\frac{1}{3}} M_\star^{\frac{5}{6}+\frac{\alpha}{2}} \sqrt{Gf}$$

The balance equation 1 then becomes:

$$\frac{\dot{a}}{a} = \frac{2}{J_{\rm orb}} \frac{dJ_{\rm orb}}{dM_\star} \dot{M}_\star + 2\beta \frac{\dot{M}_\star}{M_{\rm BH}} - 2\frac{\dot{M}_\star}{M_\star} + (1-\beta)\frac{\dot{M}_\star}{M}$$

The last equation can be integrated analytically obtaining 2 and 3.

B Fitting formulae for the maximal orbital separation

We show in Table B1 the parameters for the fitting of the maximal orbital separation as a function of the eccentricity (see expression 5).

Table B1. Fitting parameters for $a_{\rm max}$.

Source	α	β	γ	δ	ϵ
H 1705-250					
model1	8.94	-2.84	-2.43	-3.16	1.00
model 2	8.93	-2.81	-2.45	-3.16	1.00
model 3	11.00	-3.38	-2.40	-6.28	1.00
model 4	8.60	-4.70	-0.90	-4.63	1.00
model 5	7.84	-1.68	-3.94	-3.16	1.00
Nova Mus 91					
model 1	6.69	-0.79	-7.90	-3.23	1.00
model 2	6.68	-0.82	-7.24	-3.20	1.00
model 3	11.34	-7.45	-0.79	-6.32	1.00
model 4	8.20	-5.51	-0.61	-4.25	1.00
model 5	6.46	-0.68	-9.17	-3.23	1.00
GS 2000+251					
model1	8.22	-1.96	-3.49	-3.20	1.00
model 2	8.21	-1.94	-3.47	-3.18	1.00
model 3	11.01	-2.70	-3.38	-6.23	1.00
model 4	7.86	-3.69	-1.11	-4.25	1.00
model 5	7.02	-1.01	-6.26	-3.20	1.00
1A 0620-00					
model 1	7.01	-1.07	-5.86	-3.14	1.00
model 2	7.00	-1.07	-5.68	-3.12	1.00
model 3	10.80	-3.05	-2.73	-6.16	1.00
model 4	7.35	-4.22	-0.84	-3.96	1.00
model 5	6.37	-0.69	-8.77	-3.15	1.00
GRS 1009-45					
model 1	5.52	-0.53	-10.64	-2.86	1.00
model 2	5.50	-0.54	-9.99	-2.83	1.00
model 3	10.15	-3.95	-1.68	-5.79	1.00
model 4	6.69	-5.39	-0.54	-3.57	1.00
model 5	11.66	-11.20	-0.47	-6.36	1.00
GRO J0422+32					
model 1	11.73	-11.29	-0.47	-6.39	1.00
model 2	5.49	-0.54	-10.00	-2.83	1.00
model 3	9.91	-2.92	-2.55	-5.66	1.00
model 4	6.31	-3.93	-0.76	-3.41	1.00
model 5	5.20	-0.50	-10.74	-2.75	1.00
XTE J1118+480					
model 1	11.73	-11.29	-0.47	-6.39	1.00
model 2	8.68	-4.09	-0.90	-4.43	1.00
model 3	10.98	-2.25	-4.41	-6.11	1.00
model 4	6.67	-3.09	-1.14	-3.62	1.00
model 5	11.66	-11.20	-0.47	-6.36	1.00

REFERENCES

Barret D., McClintock J. E., Grindlay J. E., 1996, ApJ, 473, 963
Barret D., Olive J. F., Boirin L., Done C., Skinner G. K., Grindlay J. E., 2000, ApJ, 533, 329
Binney J., Tremaine S., 2008, Galactic Dynamics: Second Edition. Princeton University Press
Blaauw A., 1961, Bull. Astron. Inst., 15, 265
Boersma J., 1961, Bull. Astron. Inst., 15, 291
Bonnell I. A., Pringle J. E., 1995, MNRAS, 273, L12
Bowyer S., Byram E. T., Chubb T. A., Friedman H., 1965, Science, 147, 394
Brandt W. N., Podsiadlowski P., Sigurdsson S., 1995, MNRAS, 277, L35
Cantrell A. G., et al., 2010, ApJ, 710, 1127
Casares J., Jonker P. G., 2014, Space Sci. Rev., 183, 223
Casares J., Negueruela I., Ribó M., Ribas I., Paredes J. M., Herrero A., Simón-Díaz S., 2014, Nature, 505, 378
Clausen D., Piro A. L., Ott C. D., 2015, ApJ, 799, 190
Corral-Santana J. M., Casares J., Shahbaz T., Zurita C., Martínez-Pais I. G., Rodríguez-Gil P., 2011, MNRAS, 413, L15
Dessart L., Livne E., Waldman R., 2010, MNRAS, 405, 2113
Dominik M., et al., 2015, ApJ, 806, 263
Eggleton P. P., 1983, ApJ, 268, 368
Ergma E., Fedorova A., 1998, A&A, 338, 69
Fender R. P., Maccarone T. J., Heywood I., 2013, MNRAS, 430, 1538
Filippenko A. V., Matheson T., Leonard D. C., Barth A. J., van Dyk S. D., 1997, PASP, 109, 461
Filippenko A. V., Leonard D. C., Matheson T., Li W., Moran E. C., Riess A. G., 1999, PASP, 111, 969
Fragos T., Willems B., Kalogera V., Ivanova N., Rockefeller G., Fryer C. L., Young P. A., 2009, ApJ, 697, 1057
Fryer C. L., 1999, ApJ, 522, 413
Fryer C. L., Kalogera V., 2001, ApJ, 554, 548
Fryer C. L., Kusenko A., 2006, ApJS, 163, 335
Gelino D. M., 2001, PhD thesis, Center for Astrophysics and Space Sciences, University of California, San Diego ¡EMAIL¿dgelino@ucsd.edu¡/EMAIL¿
Gelino D. M., Harrison T. E., 2003, ApJ, 599, 1254
Gelino D. M., Harrison T. E., McNamara B. J., 2001, AJ, 122, 971
Gelino D. M., Balman Ş., Kızıloğlu Ü., Yılmaz A., Kalemci E., Tomsick J. A., 2006, ApJ, 642, 438
González Hernández J. I., Rebolo R., Israelian G., Casares J., Maeder A., Meynet G., 2004, ApJ, 609, 988
González Hernández J. I., Rebolo R., Israelian G., Harlaftis E. T., Filippenko A. V., Chornock R., 2006, ApJLett, 644, L49
González Hernández J. I., Casares J., Rebolo R., Israelian G., Filippenko A. V., Chornock R., 2011, ApJ, 738, 95
González Hernández J. I., Rebolo R., Casares J., 2012, ApJLett, 744, L25
González Hernández J. I., Rebolo R., Casares J., 2014, MNRAS,

438, L21
Goswami S., Kiel P., Rasio F. A., 2014, ApJ, 781, 81
Gourgoulhon E., Haensel P., 1993, A&A, 271, 187
Harpaz A., Rappaport S., 1991, ApJ, 383, 739
Heger A., Fryer C. L., Woosley S. E., Langer N., Hartmann D. H., 2003, ApJ, 591, 288
Hills J. G., 1983, ApJ, 267, 322
Hobbs G., Lorimer D. R., Lyne A. G., Kramer M., 2005, MNRAS, 360, 974
Homan J., Wijnands R., Kong A., Miller J. M., Rossi S., Belloni T., Lewin W. H. G., 2006, MNRAS, 366, 235
Hurley J. R., Pols O. R., Tout C. A., 2000, MNRAS, 315, 543
Hurley J. R., Tout C. A., Pols O. R., 2002, MNRAS, 329, 897
Hut P., 1981, A&A, 99, 126
Hynes R. I., 2005, ApJ, 623, 1026
Ioannou Z., Robinson E. L., Welsh W. F., Haswell C. A., 2004, AJ, 127, 481
Israelian G., Rebolo R., Basri G., Casares J., Martín E. L., 1999, Nature, 401, 142
Ivanova N., Taam R. E., 2003, ApJ, 599, 516
Janka H.-T., 2013, MNRAS, 434, 1355
Jonker P. G., Nelemans G., 2004, MNRAS, 354, 355
Justham S., Rappaport S., Podsiadlowski P., 2006, MNRAS, 366, 1415
Kalogera V., 1996, ApJ, 471, 352
Kalogera V., 1999, ApJ, 521, 723
Knigge C., Baraffe I., Patterson J., 2011, ApJS, 194, 28
Kochanek C. S., 2015, MNRAS, 446, 1213
Kuulkers E., et al., 2013, A&A, 552, A32
Lai D., Chernoff D. F., Cordes J. M., 2001, ApJ, 549, 1111
Lipunov V. M., Postnov K. A., Prokhorov M. E., 1997, MNRAS, 288, 245
MacFadyen A. I., Woosley S. E., Heger A., 2001, ApJ, 550, 410
Maccarone T. J., Kundu A., Zepf S. E., Rhode K. L., 2007, Nature, 445, 183
Mason K. O., Parmar A. N., White N. E., 1985, MNRAS, 216, 1033
McClintock J. E., Remillard R. A., 2006, Black hole binaries. pp 157–213
McMillan P. J., 2011, MNRAS, 414, 2446
Mihalas D., Binney J., 1981, Galactic astronomy: Structure and kinematics /2nd edition/
Miller-Jones J. C. A., 2014, PASA, 31, 16
Miller-Jones J. C. A., Jonker P. G., Nelemans G., Portegies Zwart S., Dhawan V., Brisken W., Gallo E., Rupen M. P., 2009, MNRAS, 394, 1440
Mirabel I. F., Rodrigues I., 2003, Science, 300, 1119
Morscher M., Pattabiraman B., Rodriguez C., Rasio F. A., Umbreit S., 2015, ApJ, 800, 9
Nelemans G., Tauris T. M., van den Heuvel E. P. J., 1999, A&A, 352, L87
Orosz J. A., Bailyn C. D., McClintock J. E., Remillard R. A., 1996, ApJ, 468, 380
Orosz J. A., et al., 2001, ApJ, 555, 489
Orosz J. A., McClintock J. E., Remillard R. A., Corbel S., 2004, ApJ, 616, 376
Orosz J. A., Steiner J. F., McClintock J. E., Torres M. A. P., Remillard R. A., Bailyn C. D., Miller J. M., 2011, ApJ, 730, 75
Özel F., Psaltis D., Narayan R., McClintock J. E., 2010, ApJ, 725, 1918
Paczyński B., 1971, ARA&A, 9, 183
Paczynski B., 1976, in Eggleton P., Mitton S., Whelan J., eds, IAU Symposium Vol. 73, Structure and Evolution of Close Binary Systems. p. 75
Paczynski B., 1990, ApJ, 348, 485
Parker E. N., 1958, ApJ, 128, 677
Pfahl E., Rappaport S., Podsiadlowski P., 2002a, ApJ, 573, 283
Pfahl E., Rappaport S., Podsiadlowski P., Spruit H., 2002b, ApJ, 574, 364
Podsiadlowski P., 1991, Nature, 350, 136
Podsiadlowski P., Rappaport S., Han Z., 2003, MNRAS, 341, 385
Podsiadlowski P., Langer N., Poelarends A. J. T., Rappaport S., Heger A., Pfahl E., 2004, ApJ, 612, 1044
Portegies Zwart S. F., Verbunt F., Ergma E., 1997, A&A, 321, 207
Portegies Zwart S., McMillan S., et al. H., 2009, New A, 14, 369
Pylyser E. H. P., Savonije G. J., 1989, A&A, 208, 52
Remillard R. A., Orosz J. A., McClintock J. E., Bailyn C. D., 1996, ApJ, 459, 226
Repetto S., Nelemans G., 2014, MNRAS, 444, 542
Repetto S., Davies M. B., Sigurdsson S., 2012, MNRAS, 425, 2799
Reynolds M. T., Callanan P. J., Filippenko A. V., 2007, MNRAS, 374, 657
Romani R. W., 1996, in van Paradijs J., van den Heuvel E. P. J., Kuulkers E., eds, IAU Symposium Vol. 165, Compact Stars in Binaries. p. 93
Russell T. D., Soria R., Miller-Jones J. C. A., Curran P. A., Markoff S., Russell D. M., Sivakoff G. R., 2014, MNRAS, 439, 1390
Shahbaz T., Russell D. M., Zurita C., Casares J., Corral-Santana J. M., Dhillon V. S., Marsh T. R., 2013, MNRAS, 434, 2696
Shakura N. I., Sunyaev R. A., 1973, A&A, 24, 337
Sippel A. C., Hurley J. R., 2013, MNRAS, 430, L30
Smith M. C., Ruchti G. R., et al H., 2007, MNRAS, 379, 755
Strader J., Chomiuk L., Maccarone T. J., Miller-Jones J. C. A., Seth A. C., 2012, Nature, 490, 71
Tauris T. M., van den Heuvel E. P. J., 2006, Formation and evolution of compact stellar X-ray sources. pp 623–665
Tutukov A. V., Fedorova A. V., Ergma E. V., Yungelson L. R., 1985, Soviet Astronomy Letters, 11, 52
Valsecchi F., Glebbeek E., Farr W. M., Fragos T., Willems B., Orosz J. A., Liu J., Kalogera V., 2010, Nature, 468, 77
Verbunt F., Zwaan C., 1981, A&A, 100, L7
Weber E. J., Davis Jr. L., 1967, ApJ, 148, 217
Willems B., Henninger M., Levin T., Ivanova N., Kalogera V., McGhee K., Timmes F. X., Fryer C. L., 2005, ApJ, 625, 324
Wong T.-W., Willems B., Kalogera V., 2010, ApJ, 721, 1689
Wong T.-W., Valsecchi F., Fragos T., Kalogera V., 2012, ApJ, 747, 111
Yungelson L. R., Lasota J.-P., Nelemans G., Dubus G., van den Heuvel E. P. J., Dewi J., Portegies Zwart S., 2006, A&A, 454, 559
Zhang W., Woosley S. E., Heger A., 2008, ApJ, 679, 639
della Valle M., Mirabel I. F., Rodriguez L. F., 1994, A&A, 290, 803
van den Heuvel E. P. J., 1983, in Lewin W. H. G., van den Heuvel E. P. J., eds, Accretion-Driven Stellar X-ray Sources. p. 308